ELSEVIER

Contents lists available at ScienceDirect

Ocean Engineering

journal homepage: www.elsevier.com/locate/oceaneng



Research paper

ANN-generated initial populations for PSO-based design of OWT jackets

Borja Benítez-Suárez 🕒 *, Román Quevedo-Reina 👨 , Guillermo M. Álamo 👨 , Luis A. Padrón 👨

Instituto Universitario de Sistemas Inteligentes y Aplicaciones Numéricas en Ingeniería (IUSIANI), Universidad de Las Palmas de Gran Canaria (ULPGC), Edificio Central del Parque Científico-Tecnológico, Campus Universitario de Tafira, Las Palmas de Gran Canaria, 35017, Spain

ARTICLE INFO

Keywords: Offshore wind turbine Jacket support structure Structural optimization Particle swarm optimization Finite element analysis Artificial neural networks

ABSTRACT

This paper investigates and proposes efficient strategies for generating initial populations in the automated design of jacket-type support structures for offshore wind turbines. The particle swarm optimization algorithm is employed as search and optimization method, while a finite-element-based model is used to evaluate the structural feasibility in the design process. This model computes the loads acting on the structure, assesses its structural response, and verifies key design requirements. Soil-structure interaction is also considered to account for foundation flexibility. A key contribution of this study is the use of an artificial-neural-network-based surrogate model to estimate the structural utilization factor during the initial population generation phase. Since high-fidelity evaluation is not essential at this early stage, the neural network is used for its ability to rapidly estimate the structural performance. The obtained candidates satisfy a wide range of criteria, including ultimate limit states, fundamental frequency checks, joint and geometric verifications, and foundation requirements. Several strategies are proposed for generating initial populations in a pre-optimization phase. Results demonstrate that these strategies significantly increase not only the number of feasible designs but also their quality, measured in terms of minimal material usage and compliance with design criteria. The overall algorithm performance is substantially improved.

1. Introduction

Offshore wind turbines (OWT) support structures are classified into two primary categories: fixed to the seabed and floating. The former are utilized in shallow and transitional waters up to 60 m in depth, while the latter are designed for deep waters, with a potential maximum depth exceeding 1,000 m (Arent et al., 2012). Most of the support structures for installed capacity worldwide are fixed to the seabed. Of the 68,258 MW of total installed capacity in operation worldwide, 55.6% corresponds to monopiles, while jackets account for 13.4% (McCoy et al., 2024). Monopiles are employed in shallow waters due to their ease of installation and relatively low structural cost. On the other hand, jacket substructures emerge as an alternative for transitional waters, not only for their adaptability to different soil conditions but also for their ability to withstand greater depths and more challenging environmental conditions thanks to their lattice design that efficiently distributes loads. Currently, the deepest installed OWT jacket reaches 58.6 m deep and is part of the Seagreen project in Scotland (McCoy et al., 2024). However, jacket structures have higher construction and maintenance costs due to their complex structural configuration. Currently, XXL monopiles are being developed, designed to operate at greater depths and compete with jackets at depths greater than 40 m. Ma et al. (2024) conducted a comparative study of monopiles and jackets for transitional waters, concluding that jacket-type substructures perform better than monopiles in water ranges from 30 to $60\,\mathrm{m}$.

The Global Offshore Wind Report of 2023 (Council, 2023) reveal that over the next decade, the renewable energy sector is expected to experience significant growth, with projections indicating 380 GW of new offshore wind capacity. In recent years, new offshore wind farms have been installed progressively farther from the coast, where wind resources are of better quality and where seabed depths are greater. Available data from announced projects suggest that bottom-fixed installations could reach water depths of up to 65 m in the coming years (McCoy et al., 2024). Some less optimistic analyses indicate that the current global macroeconomic context has slowed the expansion of offshore wind energy, which could lead to downward revisions in these projections. Investment costs for offshore wind projects have increased by 20 %, attributed to factors such as rising material prices, supply chain disruptions, and inflation (Bahar, 2024). On average, the cost of the support structure and foundation represents between $12\,\%$ and $20\,\%$ of the total investment in offshore wind projects (Council, 2023; Johnston et al., 2020). In addition to economic challenges, the design of these structures is characterized by a remarkable technical complexity, which requires the consideration of numerous variables and substantial computational

E-mail address: borja.benitez@ulpgc.es (B. Benítez-Suárez).

^{*} Corresponding author.

Ocean Engineering 343 (2026) 123197

effort, especially in the evaluation of the different loads acting on the structure, as well as conducting multiple verifications. Consequently, the objective of extending the structure's service life while reducing the amount of material used represents a technical challenge.

The growing ambition to increase installed offshore wind capacity, along with the interest in developing projects in deeper waters, has driven a significant increase in research focused on seabed-fixed support structures for OWT (Jiang, 2021; Wan et al., 2024; Jung and Schindler, 2023). Several studies have focused on identifying the key parameters influencing the design of substructures. Han et al. (2024) conducted a sensitivity analysis to identify key design parameters from a structural reliability perspective, specifically concerning the vibration limit state. The results showed that Young's modulus is the predominant factor, followed by the tower thickness. Additionally, they highlighted that lateral bending stiffness within the soil-structure interaction (SSI) has a significant impact on the natural frequency of the structure, emphasizing the importance of considering SSI in the structural design. Regarding loads, wind speed was identified as the most influential variable affecting tower deformation. While Han et al. (2024) focused on identifying the critical parameters affecting structural reliability in monopilesupported structures, Quevedo-Reina et al. (2024b) analyzed the global sensitivity of the fundamental frequency of OWTs supported by jackettype structures. They employed artificial neural networks (ANNs) as a surrogate model for natural frequency computation.

In the field of OWT support structure design and optimization, other researchers have directed their efforts toward the development of methodologies. In this regard, Wang et al. (2024) proposed a methodology that integrates a finite element model (FEM) for structural analysis and verification with an optimization stage, aimed at mass reduction. This optimization was carried out using two strategies: parametric optimization (PO) and genetic algorithms (GA). In the proposed case study, PO was more computationally efficient, but GA achieved better mass reduction results. Tian et al. (2024) proposed a topological optimization (TO) approach with fatigue constraints for jacket-type support structures. Based on Miner's cumulative damage criterion, the study demonstrated how this method significantly reduces the structure's mass while maintaining service life and strength requirements, ensuring its ability to withstand severe dynamic loads. To verify the effectiveness of this methodology, they used it to address the well-known OC4 reference jacket (Vorpahl et al., 2011). Ju and Hsieh (2022) proposed an optimization procedure using the Powell method, which finds the minimum value of an implicit function with multiple variables without requiring derivative calculations. This approach was applied to define the optimal geometry of the structure under extreme load conditions. The calculation model included a FEM analysis and took soil-structure interaction into account. Lu et al. (2023) applied the TO technique to tripod-type substructures, while Zhang et al. (2022) proposed a methodology focused on the conceptual design of jacket-type structures. For the latter, the approach was formulated as a multi-objective programming problem, aiming to minimize deformations and stresses in the structure, as well as its mass, under different loading conditions. The methodology began with modal and load analyses on a FEM, followed by the application of TO, which consisted in defining which parts of the structure are essential to support the loads and which are not, thus eliminating unnecessary elements and reinforcing the most critical areas. This stage respected volume and symmetry constraints, ensuring that the resulting design has realistic joints and elements. Once the optimization process was completed, loads were recalculated, and displacements and stresses were reassessed. The aforementioned studies were based on an initial jacket design, to which the described optimization techniques were subsequently applied. However, none adopt a strategy that initiates the optimization process at a conceptual stage, starting from site-specific and turbine data.

The PSO algorithm is a swarm intelligence technique inspired by the social behavior of birds and fish, developed by Kennedy and Eberhart (Kennedy and Eberhart, 1995; Eberhart and Shi, 2000). It is based on

a group of potential solutions that iteratively move through a search space to find a better position. Each candidate adjusts its position according to its own experience and that of its neighbors, enabling an effective exploration of the solution space and convergence toward local and global optima. PSO's primary strengths lie in its ability to address high-dimensional optimization problems, a domain in which traditional methods frequently encounter challenges due to their computational complexity or inefficiency. Additionally, PSO's simple implementation and independence from gradient information contribute to its notable adaptability. The efficacy of PSO in search processes can be attributed to its approach to exploration, which involves the identification of promising solutions and the subsequent refinement of these solutions to identify new regions of the solution space. This adaptability frequently results in accelerated convergence, contributing to PSO's reputation as a versatile tool across diverse domains.

In a previous study, Benítez-Suárez et al. (2025) introduced a costeffective methodology for autonomously design jacket substructures for
OWTs using a PSO algorithm coupled with a FE structural model that assumed a rigid base (i.e., disregarded the influence of SSI on the problem
at hand). Such methodology is able to generate preliminary jacket designs optimized for minimal material use while meeting structural and
geometrical requirements. A key feature for the success of the methodology was the use of pre-computed initial populations instead of the
random initial populations commonly used in PSO applications. Those
pre-computed initial populations were derived from compact design expressions by Jalbi and Bhattacharya (2020), and it was shown that they
significantly enhance the algorithm's efficiency compared to random or
mixed initial swarms, enabling faster convergence to feasible and lighter
jacket designs.

However, a more specific study on the most appropriate ways of generating such pre-computed initial populations, and a deeper understanding of their influence on the final results, are still needed. For this reason, this study aims not only at providing a more in-depth analysis of the effectiveness of various strategies for the generation of initial population strategies on the automatic optimization and design of support structures for OWT, but also at proposing and analyzing new and more effective strategies for the generation of the pre-computed initial populations through a pre-optimization step in which ANNs are used as a surrogate structural model. More precisely, this study assesses the pre-optimization step of initial populations and their influence on the design and optimization process of jacket-type support structures for OWT.

The structure of this paper is as follows: Section 2 presents an overview of the general design and optimization strategy, describes the FE structural model and the ANN surrogate model, and presents the different techniques for the generation of initial populations. The case study employed to evaluate the proposed initial populations, the results of the performance of them, and the geometrical characteristics of the resulting candidate jackets, are presented in Section 3. Finally, Section 4 summarizes the conclusions drawn from this study.

2. Methodology

2.1. Overview of the design and optimization strategy

This section aims at presenting an overview of the general design and optimization algorithm employed in this study. The ensuing sections provide a detailed discussion of certain elements of this strategy, which was originally proposed in Benítez-Suárez et al. (2025). The proposed work presents a cost-effective methodology for the autonomous design of preliminary jacket substructure candidates. Starting from metocean conditions and OWT characteristics, a set of jacket candidates is obtained reaching a sufficient level of detail for this early design phase. These candidates will subsequently serve as a starting point for more advanced design phases.

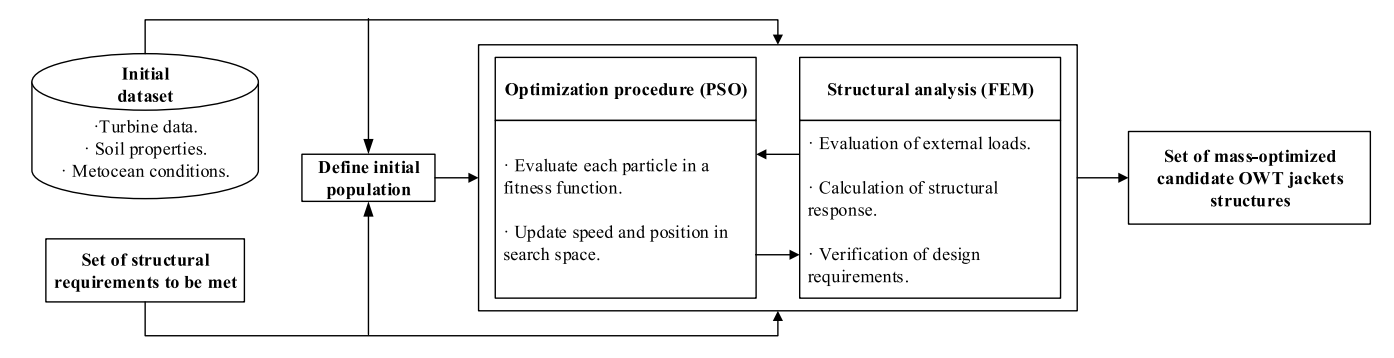


Fig. 1. Workflow for the automatic design of jacket-type OWT support structures developed by Benítez-Suárez et al. (2025).

The overall optimization routine proceeds according to the following framework:

find:
$$\vec{\phi} = \left[\phi_1, \dots, \phi_{n_{\text{var}}}\right]$$
 (1a)
mize: m_{jacket} (1b)
ct to: $\underline{\phi_i} \le \phi_i \le \overline{\phi_i}$ $i = [1, \dots, n_{\text{var}}]$ (1c)
 $\gamma_i \le \gamma_{\text{th}, i}$ $j = [1, \dots, n_{\text{reg}}]$ (1d)

to minimize:
$$m_{\text{jacket}}$$
 (1b)

subject to:
$$\underline{\phi_i} \le \phi_i \le \overline{\phi_i}$$
 $i = [1, ..., n_{\text{var}}]$ (1c)

$$\gamma_j \le \gamma_{\text{th},j}$$
 $j = [1, \dots, n_{\text{req}}]$ (1d)

where $\vec{\phi}$ is the vector containing the set of continuous design variables to be optimized of a total of n_{var} , $\overline{\phi_i}$ and ϕ_i represent the upper and lower bounds of these variables (further details are given in Section 3.1.3), m_{jacket} is the total mass of the jacket, γ_j is the utilization factor corresponding to the *j*th requirement of a total of n_{req} , and $\gamma_{\text{th},j}$ is the threshold utilization factor considered for each specific verification. The boundary values of the variables represent one of the limiting factors of the algorithm. They must be selected according to the metocean conditions, soil properties, and turbine characteristics. Wide ranges may cause the algorithm to converge more slowly to optimal solutions (local or global) and to suffer premature stagnation. Conversely, narrower boundary ranges may lead to poor exploration, potentially preventing the algorithm from finding the optimal solution. A flow chart of the design process is shown in Fig. 1.

The optimization algorithm is structured as follows: the starting point of the procedure is the input data, which can be categorized into three groups: turbine data, soil properties, and metocean conditions. Turbine data and metocean conditions are used to calculate gravitational and environmental loads (waves, tides, and wind), while soil properties enable an adequate geotechnical characterization.

The initial populations of candidates for the PSO algorithm are then generated either randomly (selecting values between the boundary values of the variables to be optimized) or through a deterministic procedure devised to obtain, with a very low computational effort, the main structural parameters of candidate designs that already take into account the most basic design concepts and requirements for this type of structures. This is achieved by a series of closed-form and simple calculations that are based on the concept design procedure of jacket foundations for offshore wind turbines in 10 steps proposed by Jalbi and Bhattacharya (2020), and that were adapted for this particular approach in Benítez-Suárez et al. (2025). This procedure begins by establishing the bending stiffness of the tower-jacket system from the system fundamental frequency's requirements. This allows to estimate the jacket's bending stiffness which, in turn, allows to compute an estimation for the required leg cross-sectional area. Diameters and thicknesses are then adjusted within a predefined range, ensuring realistic joints through geometric relations with the bracing members. The strategies for generating the initial population are enhanced in the present study through the pre-optimization of the random or deterministic initial population by a process based on ANNs, as described in Section 2.3.

The PSO algorithm is used as a search and optimization tool to find candidate jacket solutions that not only meet all the structural requirements, but do so using the minimal amount of material. To do so, the fitness function that governs the process must take into account both the structural feasibility and the weight of each particular candidate solution. The first aspect is considered through a global compliance factor for each candidate, defined as the maximum value among the partial utilization factors for each structural verification considered. Values below unity indicate that all requirements are met, whereas values above unity indicate that one or more requirements are not satisfied. These utilization factors are computed from the results obtained from the structural analysis performed using the finite element approach described in Section 2.2

The fitness function is defined as a conditional function which consists of two stages. Initially, the search process focuses on finding structurally feasible solutions that meet the utilization factor threshold. While the population does not contain a minimum percentage of particles that meet the utilization factor threshold, the fitness function output (FF_{output}) for each candidate is proportional to its global utilization factor (γ) as follows:

$$FF_{\text{output}} = \gamma \cdot \iota$$
 if $c_{\gamma} < r_{\gamma} \cdot n_{\text{particles}}$ (2)

where ι represents a penalization factor, c_{ν} is the counter tracking the number of particles within the swarm that comply with the imposed verifications, r_v is the required proportion of compliant particles prior to initiating the mass optimization phase, and $n_{\mathrm{particles}}$ are the number of particles of the swarm. This initially directs the autonomous design toward candidates that satisfy the established design criteria.

Afterwards, the effort can be redirected towards the mass minimization problem. Once a minimum number of candidates meeting the threshold utilization factor is reached, the FF_{output} shifts its focus to optimizing the mass of each candidate as follows:

$$FF_{\text{output}} = \begin{cases} m_{\text{jacket}} & \text{if} \quad \gamma \leq \gamma_{\text{th}} \\ \gamma \cdot (m_{\text{jacket}} + \delta) & \text{if} \quad \gamma > \gamma_{\text{th}} \text{ and } \gamma \leq \kappa \\ \gamma \cdot (m_{\text{iacket}} + \delta) \cdot e^{(\gamma - \kappa)} & \text{if} \quad \gamma > \kappa \end{cases}$$
(3)

where κ and δ are penalization parameters applied to individuals that do not satisfy the design constraints. The result of the process is the set of particles that constitute the swarm in the final iteration, including the candidate that best satisfies the fitness function.

The iterative process is concluded when the best solution obtained is no longer improved after a predefined number of iterations (maximum stall iterations).

The algorithm was implemented using the MATLAB programming language (version R2022.a) (The MathWorks Inc., 2022), employing the Global Optimization Toolbox (version 4.7), Deep Learning Toolbox (version 14.4), Optimization Toolbox (version 9.3), Parallel Computing Toolbox (version 7.6), Statistics and Machine Learning Toolbox (version 12.3), and Symbolic Math Toolbox (version 9.1).

2.2. Finite element structural model

This study utilizes the structural model presented by Quevedo-Reina et al. (2024c) to evaluate the feasibility of jacket structures. This model evaluates the loads acting on the jacket, computes structural response, and analyses main requirements imposed by international standards. The structural response is obtained through an equivalent static analysis assuming linear behavior. Jacket elements are represented according to Timoshenko beam theory (Friedman and Kosmatka, 1993). Rigid joints between tubular elements, and rigid connections among upper legs owing to the transition piece are assumed. Additionally, the natural frequencies of the system are obtained by solving the eigenvalue problem.

To account for the influence of pile foundation flexibility on the overall structural system, this study incorporates SSI. A surrogate model based on ANN, developed by Quevedo-Reina et al. (2024a), capable of estimating the stiffness of a pile embedded in a non-homogeneous soil is used. This ANN-based model estimates the lateral, rocking, lateralrocking coupling, and vertical stiffness of the pile from its geometry and the mechanical properties of the pile and the surrounding soil. The ANNbased model consists of an ensemble of 20 individual networks trained on a synthetic dataset of 200,000 samples generated with a numerical model (Álamo et al., 2016). The numerical model is based on the integral formulation of pile-soil interaction using Green's functions for a layered half-space, with piles represented as beam elements. It reproduces the three-dimensional linear elastic response of a pile embedded in soil, while nonlinear soil behavior is not considered. The ANN-based model shows close agreement with the numerical model, achieving absolute relative errors below 3.6% for 99% of the samples in a test dataset of 150,000 cases.

This approach neglects dynamic and pile-soil-pile interaction effects; however, the low fundamental frequency of these structures and the spacing between piles make these assumptions acceptable (Shadlou and Bhattacharya, 2016). The utilization of this surrogate model for evaluating the pile-soil interaction aims to reduce computational costs, while considering this complex and relevant phenomena in structural assessment. The estimated stiffness matrices for each pile are then incorporated into the nodes of the global stiffness matrix related to the base of the jacket legs, reflecting the foundation's flexibility.

2.2.1. Design loads

A reduced set of wind and wave load combinations, as proposed by Arany et al. (2017), is considered for the analyses. Wind conditions are defined based on load cases and turbulence definitions outlined in IEC-61400-1 (International Electrotechnical Commission (IEC), 2019). The wind load acting on the rotor of the wind turbine is assumed to be concentrated at the center of the rotor, while structural drag forces on elements above sea level are determined using DNVGL-RP-C205 (Det Norske Veritas AS, 2019c). Regarding sea loads, both wave action and marine currents are considered. Currents' velocity profile is superposed to waves' velocity profile, while the acceleration profile derives only from wave motion. The resulting drag force on submerged tubular elements is also assessed (Det Norske Veritas AS, 2019c). Gravitational loads, including the weight of all structural components (tower, Rotor-Nacelle Assembly (RNA), transition piece, among others), as well as buoyancy forces on submerged elements, are also taken into account. Additional details can be found in Benítez-Suárez et al. (2025).

2.2.2. Structural verifications

The verifications considered in this study can be grouped into three categories: ultimate limit states (ULS), fatigue limit states (FLS), and geometric constraints. This comprehensive approach ensures the structural safety and long-term performance of the substructure of the OWT. Regarding ULS verifications, the section capacity of tubular members is assessed using the von Mises yield criterion, while buckling of the members (column and shell buckling) is analyzed according to DNVGL-RP-

C202 (Det Norske Veritas AS, 2019a). Additionally, a global buckling analysis is performed. The failure of pile foundations is evaluated by verifying the section's head capacity, along with axial and lateral bearing capacities following the API Recommended Practice 2A-WSD (API, 2014).

As part of the verifications in the category of FLS, the natural frequencies of the whole structural system must always be sufficiently apart from the spectral ranges of the main dynamic actions, i.e., the 1P, the 3P and the wave excitation spectral bands. The natural frequencies are computed taking SSI into account.

Furthermore, geometric constraints are verified. This includes making sure that the minimum jacket height (DNVGL-ST-0126 Det Norske Veritas AS, 2021) is reached, and that the geometry of the welded joints follows the requirements of the DNVGL-ST-C203 standard (Det Norske Veritas AS, 2019b). Regarding the geometric constraints of piles, both the minimum pile thickness for pile installation, as specified in API Recommended Practice 2A-WSD (API, 2014), and a minimum embedded pile length, as recommended by Arany et al. (2017), are verified.

Each of the aforementioned verifications are associated with a partial utilization factor γ_j . This factor compares the actual demands imposed on the structure with its load-bearing capacity. A value of one indicates that the structure is at the limit of its capacity, while values greater than one indicate that this capacity is exceeded, meaning the verification is not satisfied.

2.3. Artificial neural network surrogate model

As stated above, one of the key steps of the aforementioned process is the generation of pre-computed initial populations composed by deterministically computed candidate solutions that already meet certain general criteria. One of the aims of this work is to perform a detailed study of these pre-computed initial populations, proposing strategies to optimize these initial sets before starting the design process. For this purpose, the surrogate model based on an ANN developed by Quevedo-Reina (2024) is used to estimate the feasibility of the jacket support structure. This model consists of a regression model that estimates the utilization factors related to the imposed structural requirements based on the most relevant characteristics of the wind turbine, the site conditions and the jacket support structure itself.

A maximum of 26 input variables are considered. The wind turbine's RNA is defined by its diameter, mass, and inertia relative to the roll and yaw axes. The tower structure includes the dimensions of the height, and diameter and thickness at both the base and top. The operating conditions are defined by the rated wind speed and the specific minimum and maximum rotor speeds. Site conditions encompass elements from wind, sea, and soil. Wind characteristics include mean velocity at 10 m above sea level and the Weibull shape parameter for wind distribution. Marine factors include water depth, circulational currents, and extreme sea states and wave heights for 1- and 50-year return periods. Soil properties involve shear wave propagation velocity, Poisson's ratio, density, and internal friction angle. Jacket component features geometric details are defined by the number of legs, number of bracing levels, height, and leg spacing at both the base and top. Tubular members of legs and braces are defined by their diameters and thicknesses from level 1 to 10. Pile dimensions are defined by its diameter, thicknesses, and length. Considered material properties are the elastic strength and the mass of the jacket platform.

The model outputs 10 partial utilization factors corresponding to the different requirements stated in Section 2.2.2. Verifications cover lateral and bearing pile capacities, pile head section strengths, section capacities, and tubular member buckling at each bracing level, for both legs and braces. Global buckling analysis is performed to confirm structural stability. FLS checks guarantee non-resonance by eliminating coincidences between natural frequencies and rotor speeds. Geometry

verifications include welded joint assessment to ensure compliance with minimum standards.

The model employs an ensemble of 20 fully connected neural networks. Each network contains 72 input neurons for capturing the problem's variables, followed by four hidden layers, each one with 200 neurons and using the ReLU activation function. The output layer comprises 26 neurons for predicting the utilization factors of each one of the imposed requirements.

The training process was performed using a synthetic dataset of 300,000 diverse samples covering a wide range of wind turbines, site conditions, and jacket designs (Quevedo-Reina, 2024). Sample generation relied on relationships among input variables defined according to international standards and case studies from the literature. Random values within these limits were assigned to each variable, and the resulting samples were evaluated using the structural model employed in this study. After training 20 individual networks, ensemble performance was tested on a dataset of 50,000 samples. The prediction of jacket feasibility achieved a Matthews correlation coefficient of 0.655, a strong result given the high imbalance of feasible (0.295%) and non-feasible (99.705%) samples in the dataset.

The ANN surrogate model thus approximates the reference model at a much lower computational cost. However, accuracy declines near the feasibility boundary, where the structural model remains necessary for reliable assessment. For this reason, the surrogate is applied in the first stage only before launching the structural model-based optimization process.

Additionally, the geometric requirements that are straightforward to evaluate are not included in the neural network's training process. These include minimum jacket height, pile thickness, and length, as well as specific ratios between diameters and thicknesses of tubular sections in the legs and braces of the structure. These requirements are assessed separately, serving as a complement to the ANN model's predictions. This dual approach enhances the overall structural analysis by combining computational predictions with direct geometric evaluations.

2.4. Strategies for the development and generation of initial populations

The aim of this section is to present the different strategies for generating initial populations that are tested and evaluated in this study. In addition to the direct strategies for generating the initial populations used in the previous study (Benítez-Suárez et al., 2025), three ANN-based strategies for refining the initial population are proposed:

 FPOP (Final POPulation): The initial pre-optimized population corresponds to the swarm resulting from the last iteration of the refine-

- ment process. Therefore, the whole pre-optimized initial population is computed after a single run of the ANN-based optimization. In this strategy, the global utilization factor threshold is set as: $\gamma_{th} = 1$.
- BEST (BEST individuals): This pre-optimized initial population is composed of the best particle obtained from independent executions. Therefore, the ANN-based optimization process is executed as many times as the number of particles needed to build the initial refined population. This strategy also considers: γ_{th} = 1.
- VUFT (Variable Utilization Factor Threshold): In this strategy, the ANN-based optimization process is also executed as many times as particles are needed to build the pre-optimized initial population but, in this case, each execution is launched with a different value of $\gamma_{\rm th}$ in a range of: $0.80 \le \gamma_{\rm th} \le 1.20$. This allows to obtain a more diversified initial population and, at the same time, partially overcomes the loss of accuracy of the ANN model in the boundary between the feasible and non-feasible regions.

Fig. 2 shows the part of the workflow that is responsible for generating the initial population of the automatic design process. Based on the three proposed strategies, a total of eight combinations are obtained. Two of them correspond to the randomized and pre-computed initial population strategies, which are applied directly in the design and optimization algorithm without being refined with the ANNs. The purpose of including these populations in the study is to provide a reference for assessing the improvement achieved by enhancing the initial populations via the ANN and to compare the candidate set obtained in the design and optimization algorithm. The remaining six combinations consist of mixtures of the three proposed pre-optimization strategies using either pre-computed or random populations as a base. Consequently, the eight considered combinations are denoted as: RNG, PC, RNG-NN-FPOP, RNG-NN-BEST, RNG-NN-VUFT, PC-NN-FPOP, PC-NN-BEST, and PC-NN-VUFT. During the pre-optimization of the initial population and for the automatic design and optimization processes, the swarm size, number of runs, fitness function, and stopping criteria are kept unchanged.

3. Results

This section analyzes the results obtained by applying the different strategies presented in the previous sections to a specific case study, based on the well known NREL-5MV reference OWT (Jonkman et al., 2009). The turbine characteristics are presented in Section 3.1.1, while the metoceanic conditions and soil properties are described in Section 3.1.2. The considered design variables are detailed in Section 3.1.3. Section 3.2 examines the influence of initial populations on the generated candidates, while Section 3.3 analyzes the main characteristics of

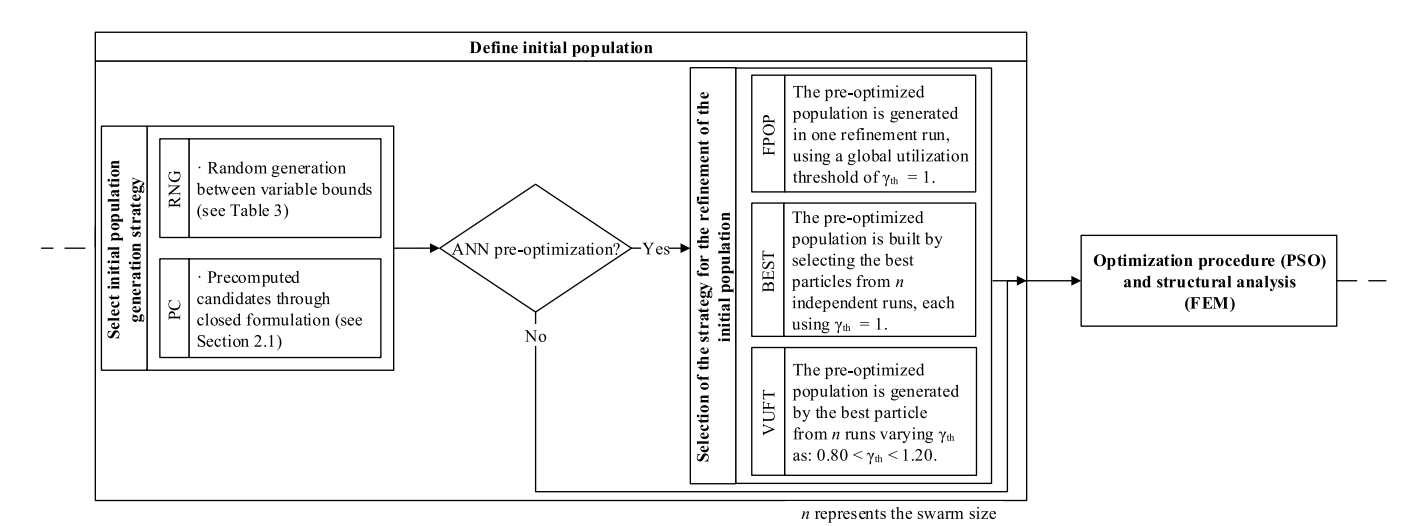


Fig. 2. Workflow for the computation of the initial population, summarizing the three tested alternatives for obtaining the pre-optimized initial populations.

the resulting candidates. Finally, Section 3.4 evaluates the computation time and the total number of iterations performed by the automatic design algorithm.

3.1. Case study

3.1.1. Wind turbine model

The NREL-5MW reference OWT model, developed by Jonkman et al. (2009), is used as a case study for testing the different strategies described above. This reference OWT has become a standard in the scientific literature for the analysis, design, and optimization of support structures for OWTs. The NREL-5MW design includes a tower height of 70 m, a hub height above mean sea level of 90.55 m, a rotor diameter of 126 m, and a rated power of 5 MW. The remaining key parameters of the turbine are detailed in Table 1.

3.1.2. Site conditions

Table 2 presents the values of the metoceanic conditions considered in the study, including wind, current, and wave data and soil properties. The wind, wave, and current conditions are those corresponding to the Dutch North Sea, as employed by Vemula et al. (2010) for the development of the OC4 reference jacket (Vorpahl et al., 2011). The soil conditions are considered to be dense sand.

3.1.3. Design variables

The optimization process considers the following variables: the diameters and thicknesses of the legs, braces, and piles, as well as the leg inclination angle. On the other hand, the number of legs and braces is defined as a fixed input parameter. A four-legged jacket is considered, with the number of braces ranging from 4 to 10. The upper spacing between the legs is set at 8 m, and the transition piece is modeled as a steel plate with a thickness of 20 cm, covering the entire upper surface

Table 1
Key parameters of the NREL 5-MW OWT (Jonkman et al., 2009).

Parameter	Value
Rating	5.0 MW
Rotor orientation	Upwind
Configuration	3 blades
Rotor diameter	126.0 m
Cut-in, cut-out, rated wind speed	3.0, 25.0, 11.4 m/s
Cut-in, rated rotor speed	6.9, 12.1 rpm
RNA mass	$3.5 \times 10^5 \text{ kg}$
Inertia RNA roll	$4.4 \times 10^7 \mathrm{kg}\cdot\mathrm{m}^2$
Inertia RNA yaw	$2.5 \times 10^7 \text{ kg} \cdot \text{m}^2$
Hub height	90.0 m
Top tower diameter	4.0 m
Top tower thickness	30.0 mm
Bottom tower diameter	5.6 m
Bottom tower thickness	32.0 mm

Table 2Environmental conditions and soil data for load calculation and soil characterization.

Variable	Value
Average wind speed at 10 m mean sea level	6.47 m/s
Weibull distribution shape parameter	2.04
1-y Extreme Sea State	7.10 m
50-y Extreme Sea State	9.40 m
1-y Extreme Wave Height	13.21 m
50-y Extreme Wave Height	17.48 m
Water depth	50.00 m
Historical average sea current velocity	0.60m/s
Shear wave propagation velocity	214.80 m/s
Soil Poisson's ratio	0.45
Soil density	$2,000.00 \text{kg/m}^3$
Internal friction angle	33.00 deg

 Table 3

 Continue design variables and their boundary values.

Variable (ϕ_i)	Lower bound $\left(\underline{\phi_i}\right)$	Upper bound $\left(\overline{\phi_i}\right)$
α_{leg} [deg]	0.50	10.00
$D_{\log,i}$ [m]	0.30	3.00
$D_{\mathrm{br},i}$ [m]	0.06	3.00
$t_{\text{leg}, i}$ [mm]	4.00	180.00
$t_{\text{br}, i}$ [mm]	0.90	180.00
$D_{\rm pile}$ [m]	0.20	4.00
t _{pile} [m]	0.01	0.25
\hat{L}_{pile} [m]	15.00	60.00

of the jacket. The continuous variables are represented by the vector $\vec{\phi}$, defined as follows:

$$\begin{split} \vec{\phi} &= \left(D_{\text{leg},1}, \, t_{\text{leg},1}, \, D_{\text{br},1}, \, t_{\text{br},1}, \, \dots, \, D_{\text{leg},n_{\text{br}}}, \, t_{\text{leg},n_{\text{br}}}, \, D_{\text{br},n_{\text{br}}}, \, t_{\text{br},n_{\text{br}}}, \, \alpha_{\text{leg}}, \\ D_{\text{pile}}, \, t_{\text{pile}}, \, L_{\text{pile}} \right) \in \mathbb{R}^{n_{\text{var}}} \end{split}$$

where D_{\square} and t_{\square} the outer diameter and thickness of the tubular sections (legs, braces and piles), $L_{\rm pile}$ is the embedded length of the pile, and $\alpha_{\rm leg}$ is the angle of inclination of the legs with respect to the vertical. The diameter and thickness of the legs and braces are defined at each brace level. Table 3 shows the upper and lower limits of the vector $\vec{\phi}$. The variables are continuous and are defined to provide sufficiently wide ranges that can represent all possible solutions, while remaining within realistic margins. Also, it is ensured that these ranges are within those used to train the structural surrogate model.

Regarding the material properties, the yield strength of steel is considered to be 350 MPa, the elastic modulus is set at 210 GPa, Poisson's ratio is taken as 0.30, and the steel density is assumed to be 7.850 kg/m^3 .

The algorithm implementation requires the definition of several key parameters. The swarm size is set to 40 particles. The stopping criterion is triggered after 10 consecutive iterations in which there has been no improvement in the fitness function. The procedure is repeated four times for each brace level and for each initial population generation method, resulting in a total of 224 runs. Finally, the values of the fitness function parameters, which are assumed to be the same as proposed in Benítez-Suárez et al. (2025), are defined as follows: $r_{\gamma}=0.1$, $\iota=10^{10}$, $\kappa=1.50$, and $\delta=10^7$.

3.2. Performance analysis of different initial populations in the optimization process

The purpose of this section is to analyze the different strategies proposed to generate the initial populations. Firstly, to analyze the quality of the populations obtained from each strategy, Fig. 3 presents a horizontal bar chart illustrating, in green, the percentage of initial populations that contain one or more particles that meet all the design requirements and, in red, the percentage of initial populations for which all particles fail to meet all or any of the design requirements. This information is given for each one of the different methodologies tested for the generation of the initial populations. For each proposed methodology, a total of 28 initial populations are considered, derived from the 7 evaluated bracing levels, with 4 algorithm repetitions per level. Once the particles of the 28 initial populations were obtained, they were evaluated using the FE model to assess their fitness with respect to the design criteria and to determine the global utilization factor of every candidate structure.

The first conclusion that can be drawn from this result is that the only methodologies able to generate initial populations that already contain at least one feasible structural particle are those that involve an initial pre-computed population that is further refined through the ANN-based optimization. The other alternatives (all randomly-generated populations, even if they are later refined with ANNs, and the initial pre-computed populations) do not contain any feasible structure. This result is attributed to two main factors: a) although the simplified formulation proposed by Jalbi and Bhattacharya (2020) does not take into account

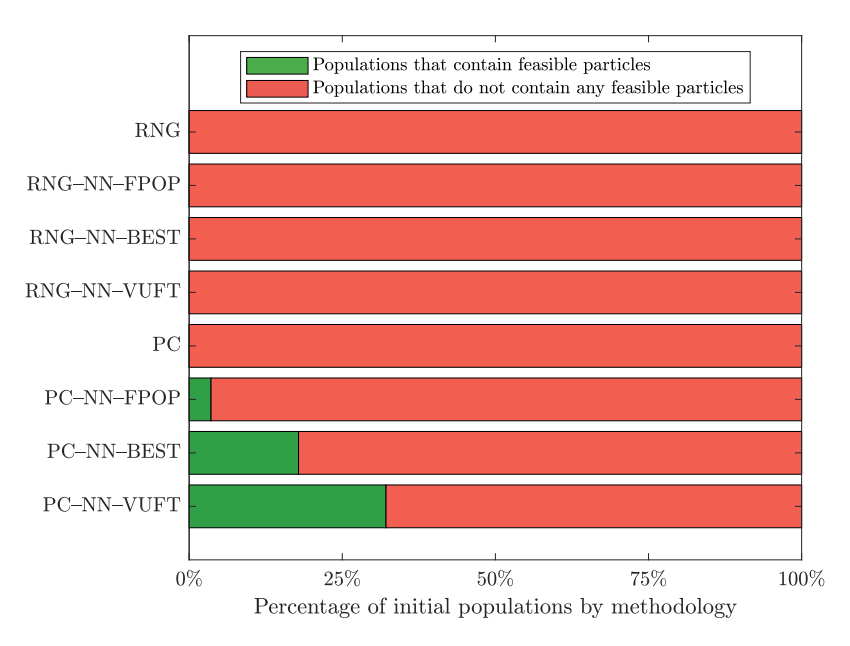


Fig. 3. Percentage of initial populations containing one or more particles that satisfy the design requirements (green bars) and those that do not (red bars), categorized by the initial population generation method.

environmental conditions and soil characterization, it is able to effectively constrain the design problem, and b) the proposed ANN-based methodology for the refining of the initial populations is able to adequately lead the optimization process to feasible solutions if the starting population already takes into account basic structural relationships (as it is the case with the pre-computed initial populations). Therefore, the use of the ANN-based surrogate model to pre-optimize the particles enhances the design process, as the algorithm is able to identify feasible solutions. The VUFT strategy is identified as the one able to produce the largest number of initial populations that already include feasible particles, reaching a proportion that almost doubles that obtained with the BEST strategy. Since the threshold utilization factor (γ_{th}) is changed during the VUFT strategy, the error arising from evaluating particles in the ANNs at the boundary between feasible and non-feasible solutions can be mitigated. On the contrary, with the FPOP strategy, very few initial populations include any feasible particles.

In order to identify which structural verifications are limiting the design in the generation of the initial population, Fig. 4 shows a set of distributions, one for each proposed strategy, with the box-and-whisker plot of the fulfillment of each one of the structural verifications separately. The results presented herein encompass all particles for all initial populations. The region where the partial verifications meet the design requirement ($\gamma_i \le 1$, highlighted in green) and the region where the requirements are not met $(\gamma_i > 1$, highlighted in red) are indicated. The verifications of each graphic are detailed as follows: the first verification corresponds to the fatigue limit state (Natural frequency), followed by the soil bearing capacity (Soil capacity). Next, the ultimate limit states of the pile (ULS pile), legs and braces (ULS of the leg and braces from the 1st to the 10th level) are represented. Subsequently, the global buckling check (Global buckling) and the verification of the pile's active length (Minimum pile depth) are included. Finally, the checks related to the minimum pile thickness for pile installation (Minimal t/d), the jacket height (Jacket height), and the verification of jacket basic geometrical requirements are presented (Geometric checks). For further details on the design criteria and verifications, refer to Section 2.2.2.

The partial utilization factor corresponding to the verification on the admissible frequency range for the fundamental frequency of the system jacket-OWT has a significant impact on the design, being the one that presents the least dispersion in all strategies. The different levels of legs and braces exhibit a decreasing trend in terms of the average value of

the material utilization factor. The bottom level of the jacket (the one in contact with the seabed) is labeled as level 1, while the highest level may range from level 4 (if the jacket has 4 braces) to level 10 (if it has 10 braces). As observed, the partial utilization factor for the lower sections of the structure approaches the threshold value. This is due to higher demands for this levels compared to the upper ones.

In general terms, the initial populations using the pre-computed strategy exhibit less dispersion in the partial utilization factors compared to their randomly generated counterparts. Moreover, the average utilization factors are closer to the threshold value, which indicates a more effective optimization process and suggesting that the increased constrains yield improved results. The use of pre-computed initial populations refined with ANNs successfully overcomes the first stage of the conditional objective function, where the optimization process aims to obtain particles that meet the design requirements, without considering the jacket mass.

After analyzing the compliance of the initial populations, the focus is shifted to the candidate solutions obtained after the design process. First, the best candidates (defined as those with the lowest mass and full compliance with the design requirements) will be studied. Then, the global utilization factor and masses of all generated candidates will be analyzed. In all cases, the analysis will distinguish between the different strategies used to generate the initial populations, whether preoptimized or not.

Fig. 5 shows a diagram with four distribution bars, each corresponding to the top five, top ten, top twenty-five, and top fifty candidates obtained after the design and optimization process. All represented candidates meet the design requirements. The order is established from lower to higher mass of the jacket structures. Pre-computed initial population generation methodologies are represented using warm colors, while random methodologies are indicated with cool colors. The vertical axis represents the percentage of candidates obtained by each type of initial population generation strategy. Across all bars in the diagram, a notable presence of warm colors is found, indicating that the best candidates are obtained based on pre-computed and pre-optimized initial population generation strategies. Among the strategies using random pre-populations, the RNG-NN-FPOP and RNG-NN-BEST methodologies stand out as those yielding the highest-quality candidates.

It is worth noting that the best candidate was obtained using the PC-NN-BEST strategy. Regarding the different braces, the best 4-braced

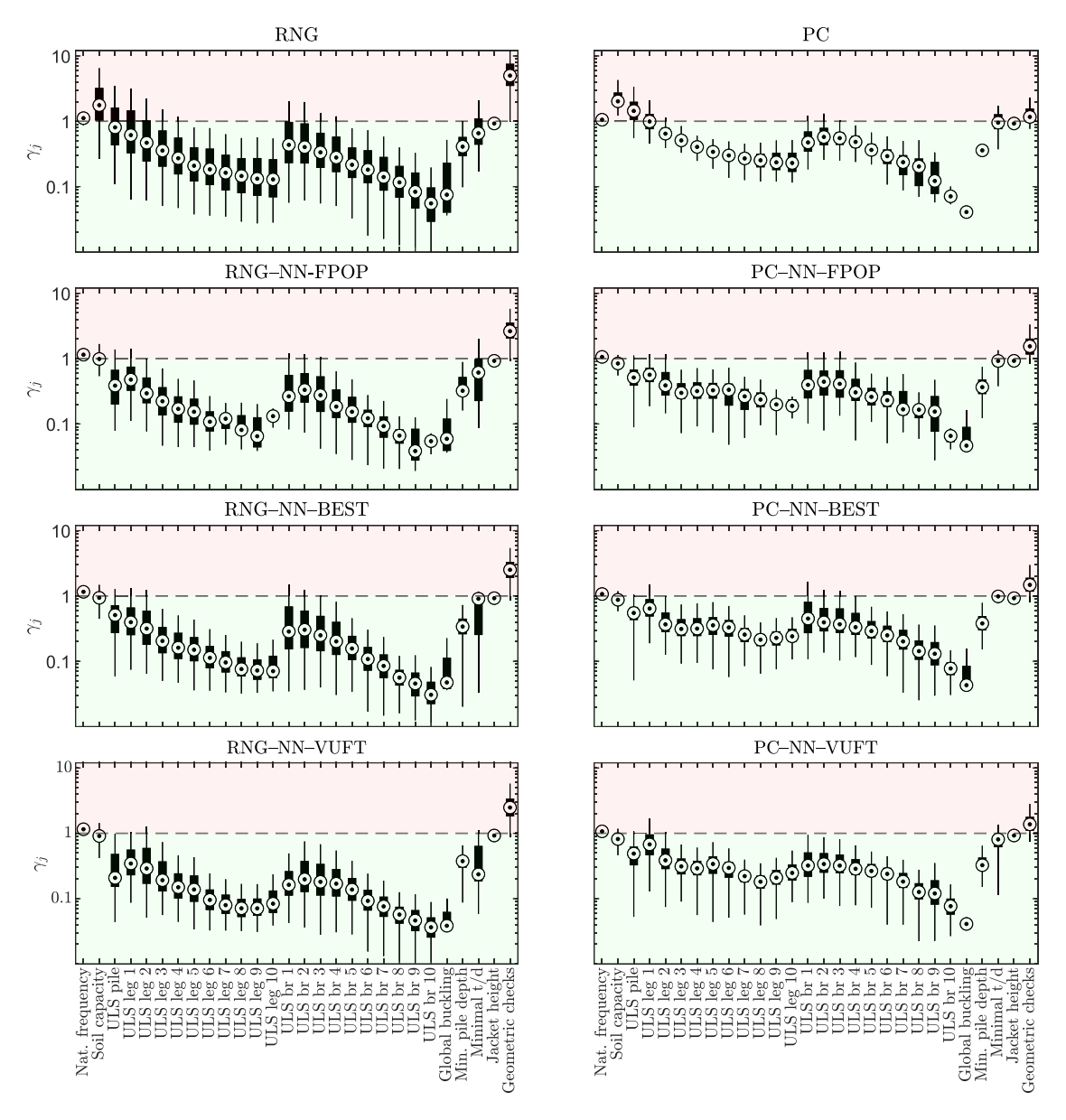


Fig. 4. Distribution of the partial utilization factor for each methodology, corresponding to the structural verifications and considering all particles and all initial populations.

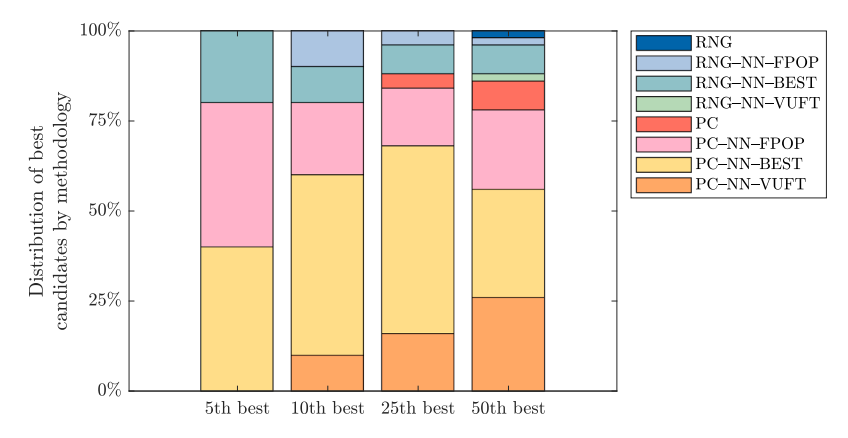


Fig. 5. Distribution of top candidates according to different initial populations strategies. Warm colors denote pre-computed methods, cool colors indicate random-based approaches.

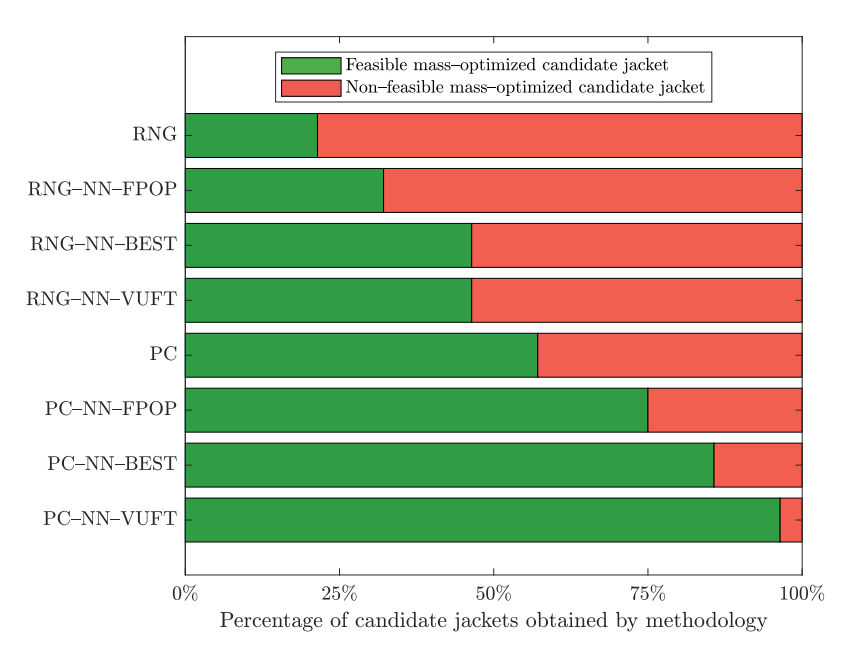


Fig. 6. Percentage of mass-optimized jacket candidates that meet the design requirements (green bars) and those that do not (red bars), distributed by initial population generation methodology.

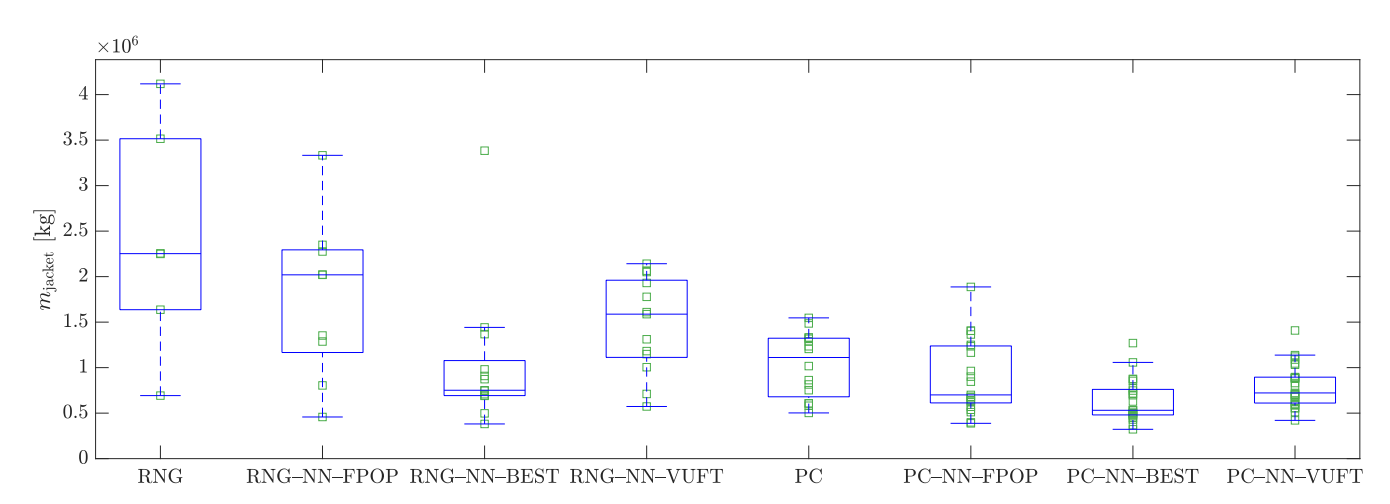


Fig. 7. Masses of candidates that meet the design requirements depending on the strategy used to determine the initial population.

candidate was obtained using the PC-NN-FPOP strategy, while the others 5-, 6-, 7-, 8-, 9-, and 10-braced candidates were generated with PC-NN-BEST strategy.

An analysis of the overall compliance factor is shown in Fig. 6, for the mass-optimized candidates obtained through the different proposed strategies. The horizontal axis indicates the percentage of candidates that meet (in green) and do not meet (in red) all the established design requirements. The results indicate that methodologies based on precomputed initial populations, whether pre-optimized (PC-NNN-FPOP, PC-NN-BEST, and PC-NN-VUFT) or not (PC), consistently yield a higher number of feasible candidates compared to those based on random populations, whether pre-optimized (RNG-NNN-FPOP, RNG-NN-BEST, and RNG-NN-VUFT) or not (RNG). For the automatic design algorithm using random populations, the percentage of feasible candidates ranges from 21 % to 46 %. In contrast, pre-computed populations yield a range between 57 % and 96 %. When these pre-computed populations are subjected to a pre-optimization process using the ANNs, the percentage further improves, ranging from 75% to 96%, representing a notable increase in the number of feasible candidates generated.

Fig. 7 presents the distribution of the mass of the candidates obtained in the optimization algorithm, for each initial population generation.

ation strategy. Additionally, the results are overlaid as individual points to facilitate the visualization of the distribution. It is important to note that the data represented correspond exclusively to candidates that meet all the established design requirements.

In general, the use of pre-computed populations significantly improves the results obtained, not only in terms of the number of feasible candidates, as previously mentioned, but also in the quality of these candidates. Notably, initial populations pre-optimized with ANNs, particularly those based on previously pre-computed populations, exhibit lower mean masses than non-optimized pre-computed populations. In this regard, the use of ANNs in the pre-optimization of initial populations demonstrates enhanced performance in the design and optimization process.

3.3. Analysis of the obtained candidates

This section presents a detailed analysis of the candidates obtained during the design process, aiming to identify the most significant geometric relationships. The purpose of this study is to evaluate the consistency of the results with established trends and standards for jacket-type support structures.

Ocean Engineering 343 (2026) 123197

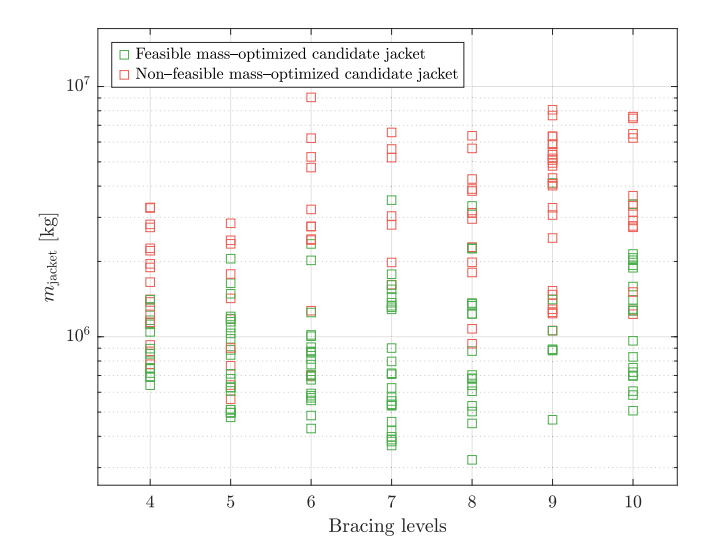


Fig. 8. Masses of feasible and non-feasible jackets for different bracing levels. The red squares indicate designs that do not meet the established design requirements, while the green ones signify feasible solutions.

Fig. 8 shows the mass of the obtained candidates in the autonomous design and optimization algorithm. The red squares indicate designs that do not meet the established design requirements, while the green ones represent feasible solutions. For the environmental conditions and the specifications of the wind turbine of the case study (see Tables 2 and 1), the results regarding the number of braces follow a trend where the lighter configurations are around 8 braces. Both a higher number of braces (increased number of elements) and a lower number (reduced structural stiffness, forcing an increase in the cross-sectional areas of the legs to withstand the forces) result in less competitive designs in terms of mass. The best result obtained achieves a mass of 322.21 tons, with a geometric configuration of 8 braces and a global compliance factor of $\gamma=0.992$.

Fig. 9 shows a three-dimensional representation of the best candidates by brace level, where the cross-sectional area of each member is represented on a color scale. The distribution of cross-sectional areas in the members of a jacket is primarily determined by the structural demands associated with operational and environmental loads. Areas with larger cross-sections (indicated by warmer colors) are concentrated at the base of the legs and in the wave impact region. These areas experience the most significant stresses, derived from both the vertical loads caused by the weight of the wind turbine and the structure, as well as those induced by the horizontal forces corresponding to waves, ocean currents, and wind. For a high number of braces, the trend of assigning larger cross-sectional areas to the legs and braces located in the upper and lower regions of the jacket is not followed. In this case, the design and optimization process includes a greater number of bars in the set of design variables, which may lead to premature algorithm convergence.

One of the variables used in the design is the angle of inclination of the jacket legs, denoted as $\alpha_{\rm leg}$. Fig. 10 plots $\alpha_{\rm leg}$ and the masses for the candidates that meet the design requirements. The angle is computed as $\alpha_{\rm leg}=\arctan(\left(S_{\rm base}-S_{\rm top}\right)/\left(\sqrt{2}\cdot H_{\rm jacket}\right))$, being $S_{\rm base}$ the distance between legs at the base, $S_{\rm top}$ the top leg spacing, and $H_{\rm jacket}$ the jacket height. The average angle of inclination of the legs for all cases that meet the design requirements is around 3.1°. In Fig. 10, an increasing trend of the batter angle can be observed as the mass of the candidates obtained decreases. A higher batter angle implies a longer leg length and, consequently, an increase in the lever arm available to resist the stresses. In that sense, the automatic design algorithm effectively balances jacket mass and the angle of inclination of the legs.

One of the parameters associated with variables of the design algorithm is the brace inclination angle $\beta_{\rm br}$. This angle remains con-

stant for all reinforcement levels, with the height of the braces varying at each level. The angle is obtained using the expression proposed by Jalbi and Bhattacharya (Jalbi and Bhattacharya, 2020) $\beta_{\rm br}=\arctan((m-1)/((m+1)\cdot\tan(\alpha_{\rm leg})))$, where $m=\left(S_{\rm bottom}/S_{\rm top}\right)^{(1/N_{\rm br})}$, being $N_{\rm br}$ the number of braces. Fig. 11 shows the mass and the $\beta_{\rm br}$ for all jacket candidates that meet the design requirements. For lattice structures, the most common range for this angle is between 30° and 60° (API, 2014; Det Norske Veritas AS, 2014). In the obtained results, the average angle is 36.02°.

To analyze the influence of the number of braces, Fig. 12 presents the distribution of the batter angle of the legs (a) and the brace inclination angle (b) for each brace number and for the candidates meeting design requirements. The black boxes in (b) represent the boundaries of the brace inclination angle. The upper and lower limits depend on the angle of inclination of the legs (see the limits of the $\alpha_{\rm leg}$ variable in Table 3). The mean of the batter angles tends to decrease as the number of braces increases, suggesting that the increase in structural stiffness results from the greater number of braces rather than the leg inclination. Similarly, the mean brace angles also decrease as the number of bracings increases. It is worth noting that the brace angle is directly dependent on both the number of braces and the batter angle of the legs.

Finally, the fundamental frequency of the candidates is studied. Considering the rotor rotational speeds (see Table 1), the 1P range is determined to be between 0.115 and 0.202 Hz, while the 3P range lies between 0.345 and 0.605 Hz. The wave excitation frequency is computed based on the wave period, which is obtained according to the standard DNVGL-ST-0437 (Det Norske Veritas AS, 2024), using the following expression:

$$11.1\sqrt{\frac{h_{\text{wave}}}{g}} \le T_{\text{wave}} \le 14.3\sqrt{\frac{h_{\text{wave}}}{g}} \tag{4}$$

where $h_{\rm wave}$ is the wave height and g the acceleration due to gravity in $\rm m/s^2$. Thus, it is established that the wave excitation frequency range lies between 0.05 and 0.106 Hz. Therefore, to ensure proper structural behavior against vibrations, the natural frequency of the jacket must fall within the 1P-3P interval, i.e., from 0.202 to 0.345 Hz.

Fig. 13 presents the distribution of the fundamental frequency of the candidates that meet the design requirements, for different brace levels. Additionally, the 1P and 3P boundary limits are indicated, regions that the jacket-OWT system must avoid to prevent resonance (highlighted red zone in the figure). These limits are displaced owing to the $\pm 5\,\%$ uncertainty established in the DNV-ST-0126 (Det Norske Veritas AS, 2021). The operating range is set between 0.212 and 0.328 Hz. It can be observed that designs with 4 and 10 braces exhibit, on average, greater stiffness than those with intermediate levels. With fewer braces, the algorithm tends to stiffen the structure to withstand the loads, while as the number of braces increases, the structure becomes more rigid by design. Greater dispersion in frequency is seen for intermediate configurations (e.g., with 7 to 9 braces), suggesting a higher sensitivity to design parameters in these configurations.

It is noteworthy that the autonomous design and optimization algorithm demonstrates notable performance in generating solutions that meet the imposed requirements, in terms of stresses, geometric verifications, and fundamental frequency limits. Partially, this accomplishment can be attributed to the employment of sophisticated initial population generation strategies proposed in this paper.

3.4. Computing time

This section evaluates the time required and the total number of iterations used by each case during the automatic design and the generation of the initial population. The study was conducted on a computing cluster that allowed the parallelization of 40 processes (equivalent to the number of candidates) using two Intel Xeon Platinum 8362 processors with 256 GB of RAM. The total computation time depends on several

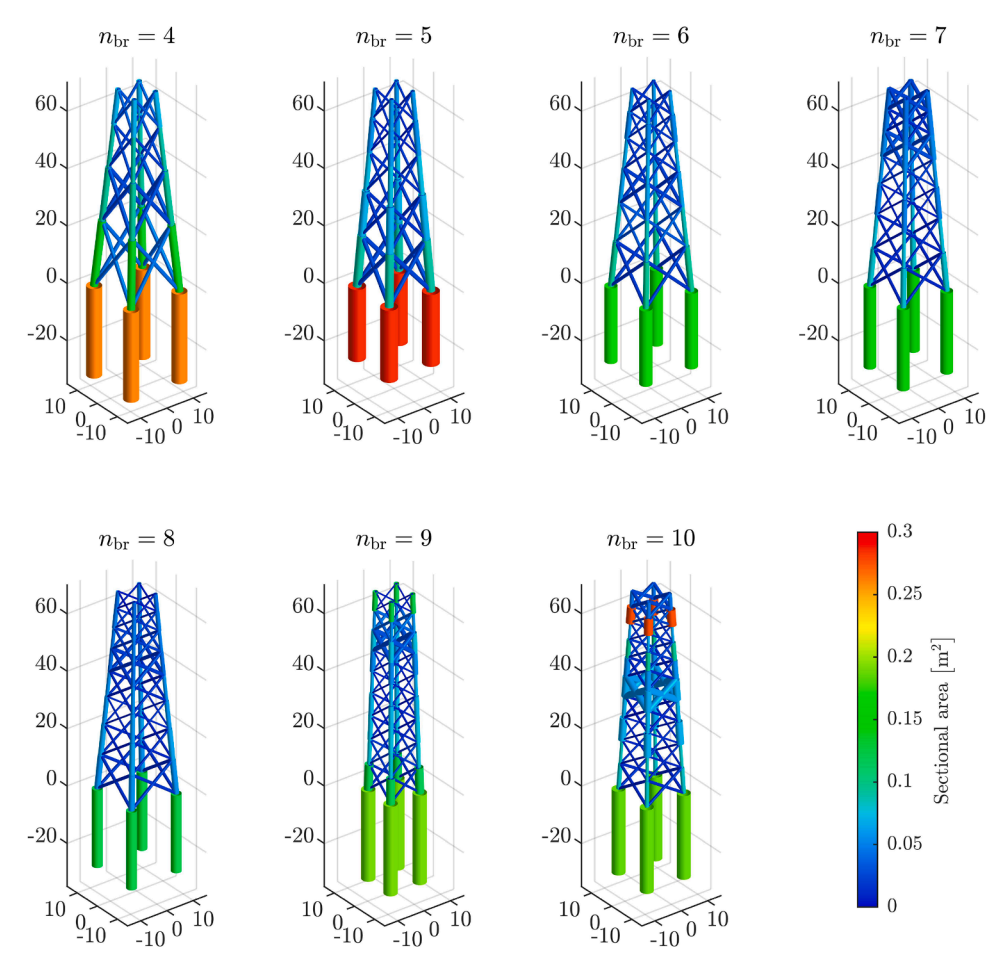


Fig. 9. Representation of the best candidates, categorized by brace level. Lengths are expressed in meters.

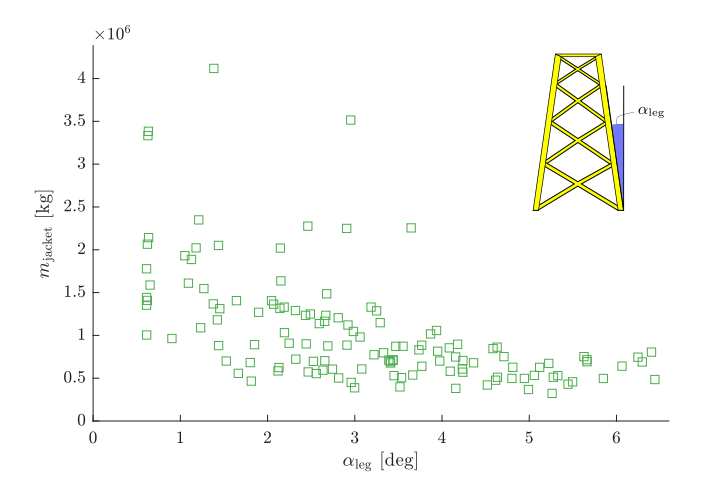


Fig. 10. Distribution of leg batter angles and jacket mass for candidates meeting the design requirements.

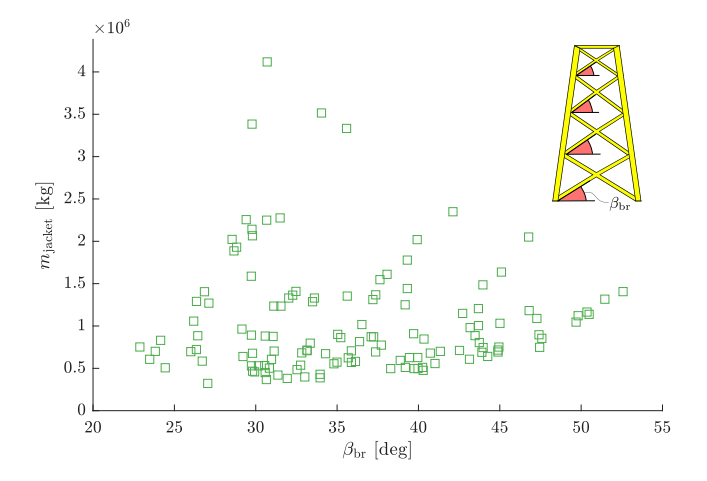


Fig. 11. Distribution of bracing angles (constant for all levels) and mass for candidates meeting all the design requirements.

factors, primarily the total number of iterations, the number of bars or elements to be analyzed, and PSO-related processes such as updating the velocity and position of the candidates at each iteration, among others. Therefore, processes that require a higher number of iterations or involve jackets with a greater number of legs or braces require more time, both in FEM analysis and in the overall design process.

Fig. 14 presents a distribution of the total computation time for each initial population generation strategy. The blue boxes represent the time

spent on the automatic design and optimization process (only candidates that meet the design requirements are considered), while the black boxes indicate the time required for the generation of the initial population. Partial data are also shown as green squares to illustrate their dispersion, but only for the autonomous design process.

In general, pre-computed populations require, on average, less time than randomly generated ones, and their behavior is, in general terms, superior (they offer a greater number of candidates and, as previously

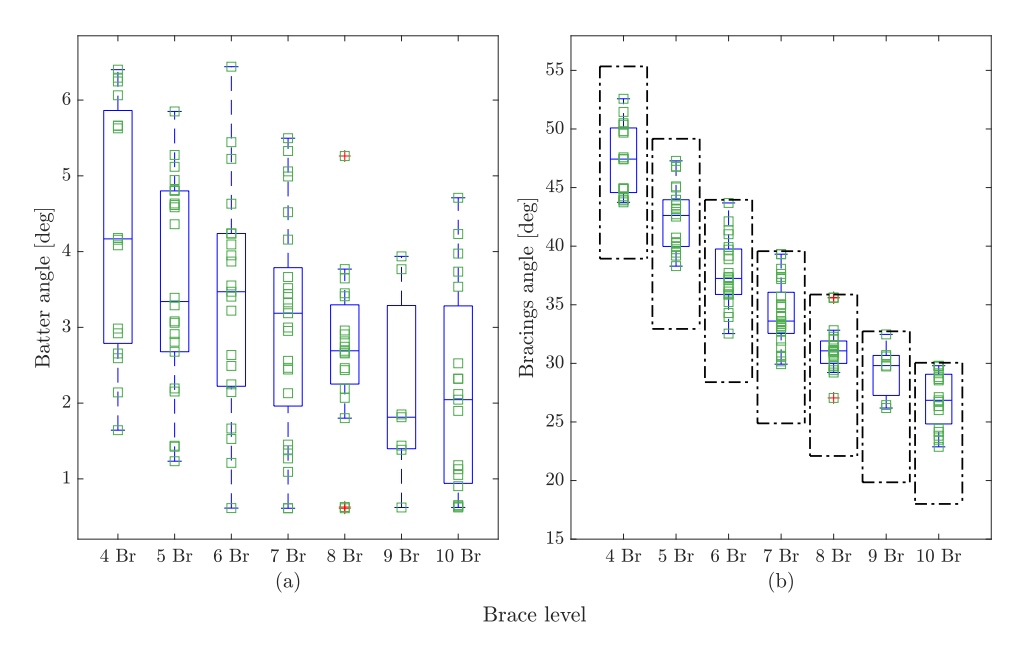


Fig. 12. Distribution of the angle of inclination (a) and the angle of inclination of the braces (b) for each brace level. The boxes in (b) represent the range of the brace angle.

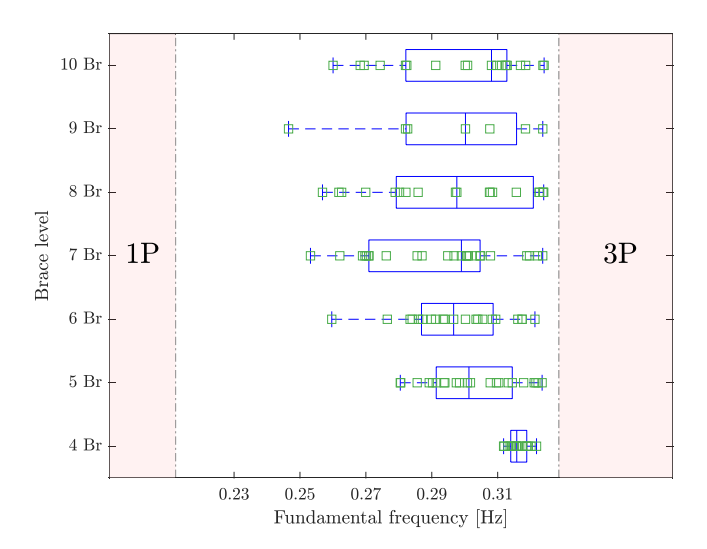


Fig. 13. Distribution of the system fundamental frequency by brace level.

discussed, of higher quality). As has been previously noted, the computational effort required for pre-computed populations is minimal when compared to the results obtained (in term of mass and compliance with verifications). However, this type of initial population can lead to a stagnation of the algorithm and to higher computational times, which results in a greater dispersion of results and computational times. As can be seen in Fig. 14, the impact of ANNs on the total computational time is minimal, but their efficiency is very high. Consequently, the exclusion of ANN-based pre-optimization initial populations reduces the competitiveness of the algorithm.

Table 4 summarizes, for each strategy, the number of feasible and non-feasible candidates, the total mean simulation time, and the average time required by the algorithm to obtain a feasible solution. All cases using random (RNG) pre-populations, whether optimized or not, require longer computation times to achieve feasible results. For these cases, the use of ANNs to pre-optimize the initial populations reduces the computational effort needed to obtain feasible solutions. Nevertheless, strategies based on RNG populations still demand more computational

Table 4Computational performance of the different proposed strategies.

Strategy	Feasible candidates	Non-feasible candidates	Mean total time [min]	Mean time to get a feasible solution [min]
RNG	6	22	361	1685
RNG-NN-FPOP	9	19	382	1188
RNG-NN-BEST	13	15	340	732
RNG-NN-VUFT	13	15	414	892
PC	16	12	287	502
PC-NN-FPOP	21	7	327	436
PC-NN-BEST	24	4	459	536
PC-NN-VUFT	27	1	343	356

resources compared to cases employing pre-computed (PC) populations. For the PC strategies, the computational improvement achieved by pre-optimizing the initial populations is less pronounced than in RNG pre-populations. In fact, for the PC-NN-BEST strategy, the computational performance worsens slightly, but this is balanced by the increase in feasible solutions obtained.

The best-performing strategy, yielding the lowest time to get feasible solutions, is PC-NN-VUFT. This result is reinforced by the fact that this strategy also achieved the highest number of feasible solutions. Conversely, the worst-performing strategy, in terms of computational effort to obtain feasible solutions, is, as expected, the one based on fully RNG non-optimized initial populations. This is further supported by the fact that this strategy resulted in the lowest number of feasible solutions found.

Finally, Fig. 15 shows a distribution of the total number of iterations employed by each candidate that meets the design requirements during the automatic design process, according to the initial population generation strategy. The trends observed are similar to those in Fig. 14: strategies based on previously computed initial populations tend to require a lower average number of iterations compared to random ones, although the maximum values are comparable. The reduced number of iterations in strategies with pre-computed initial populations reflects a greater efficiency of the automatic design algorithm in locating higher-quality candidates (lower mass and meeting the design requirements).

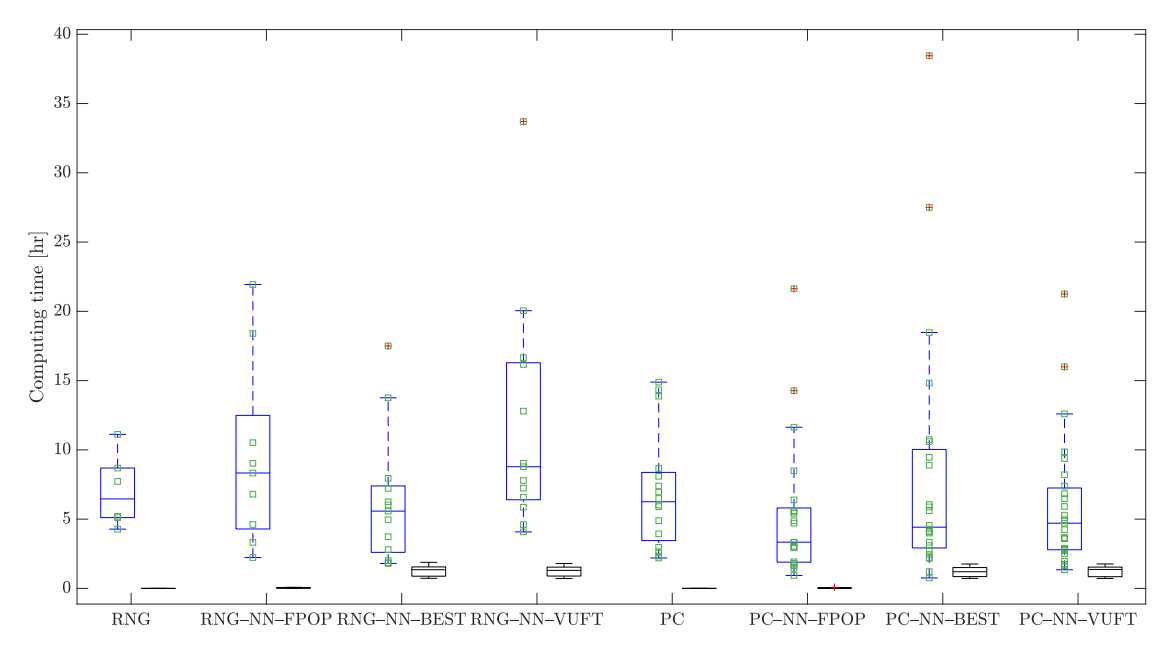


Fig. 14. Computation time for the whole optimization process (blue boxes) and for the initial population generation (black boxes). Only runs that generated feasible candidates are presented.

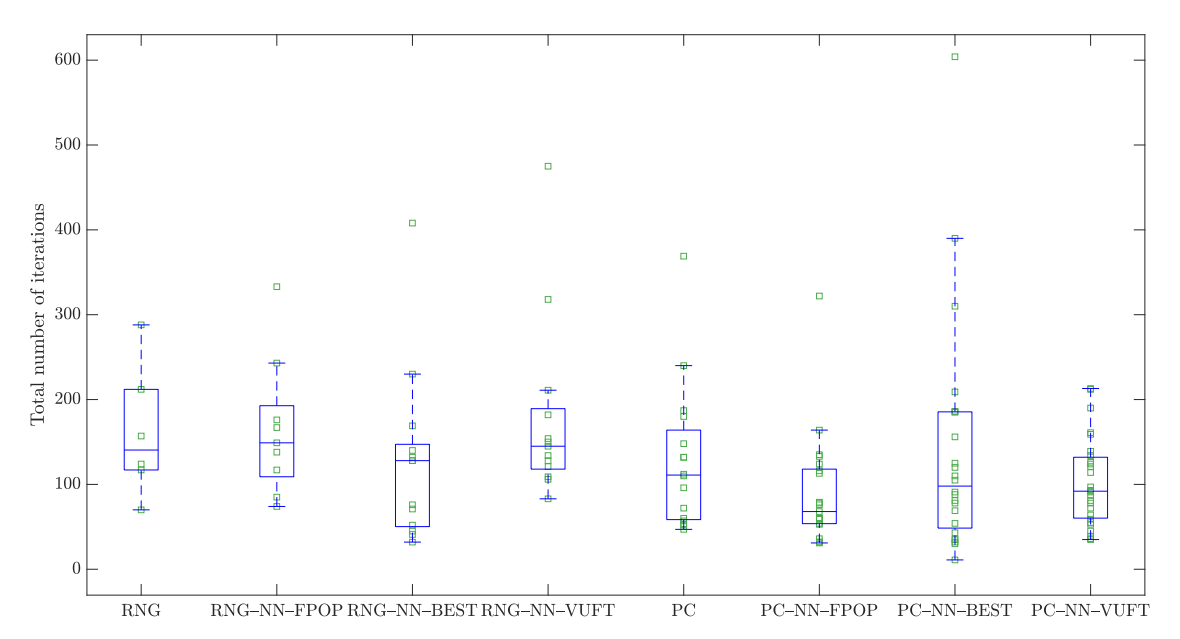


Fig. 15. Total number of iterations for each strategy. Only runs that generated feasible candidates are presented.

4. Conclusions

In a previous work (Benítez-Suárez et al., 2025), a methodology was presented that is capable of autonomously design and optimize jacket-type support structures for OWT. For this purpose, the PSO metaheuristic algorithm was coupled with a FE structural model. The methodology allows for the development of preliminary jacket designs based on metocean conditions, soil characterization, and wind turbine specifications. Compared to other optimization strategies, it does not require an initial concept to begin the process. Another key feature of the approach is the use of deterministically computed candidates as initial populations, which significantly enhances the performance of the design and optimization procedure.

In the present work, an in-depth study is made to determine suitable methods for generating initial populations and to assess their impact on the design and optimization process. To address this, the present work proposes a pre-optimization process for the initial populations using a surrogate model based on ANNs for estimating the utilization factor.

The proposed approach consists of pre-optimizing an initial set of particles, either random or deterministically computed candidates, using a procedure based on PSO coupled with an ANN as a surrogate model. Three methodologies have been developed to generate the initial populations. Based on these three methodologies and the application of ANN-based pre-optimization, eight different configurations are evaluated. These include combinations with and without pre-optimization, using either random or pre-computed initial populations. The study of the different strategies proposed for the development of the initial populations leads to the following main conclusions:

Only the initial populations that use pre-computed optimized populations included particles meeting the design requirements. The strategy that yields the greatest number of particles that meet the design

requirements is the strategy that varies in the fitness function the threshold utilization factor and use the pre-computed pre-population (PC-NN-VUFT). This strategy allows to obtain a more diversified and rich refined initial population.

- Pre-computed initial populations, compared to their random counterparts, exhibit lower dispersion in the partial utilization factors of the different design verifications, indicating that the use of pre-computed pre-populations successfully overcomes the first stage of the conditional objective function, where the optimization process aims to obtain particles that meet the design requirements. The verification related to the admissible frequency range for the fundamental frequency shows the lowest dispersion across all strategies.
- Refining the initial populations significantly improves the obtained candidate designs. In the pre-optimized strategies, 64% of the candidates meet all design requirements, whereas in the non-pre-optimized ones, only 39% fulfill these requirements. In the case of pre-computed populations (regardless pre-optimized or not), 78.6% of the candidates meet all design requirements, whereas for randomly-generated once (pre-optimized or not), only 36.6% of the candidates satisfy the design requirements.
- The best candidate obtained by the automatic design and optimization algorithm corresponds to the strategy that conducts the ANN-based optimization as many times as the swarm size. Among the 10 best candidates, all of them were obtained using ANN-optimized populations. Of these, 8 were obtained using pre-computed initial populations, while the remaining 2 resulted from the use of random populations.
- Pre-optimized initial populations using ANNs significantly enhance candidate quality and overall algorithm performance, with minimal computational cost. Excluding ANN-based pre-optimization notably reduces the algorithm's competitiveness, despite potential increases in runtime variability.

After analyzing the conceptual jacket candidates obtained from the different initial population generation strategies for the reference 5-MW OWT case study, it is found that:

- On average, the jackets with the lowest mass were the 8-brace configuration. Jackets with a higher number of elements, as well as those with fewer braces (which require an increase in cross-sectional area to ensure structural stiffness), were found to be less competitive.
- The mean angle of inclination of the legs is $\alpha_{leg}=3.1^{\circ}$. The average brace inclination angle is $\beta_{br}=36.02^{\circ}$, which is in line with the recommendations of international organizations and standards (API, 2014; Det Norske Veritas AS, 2014), which recommends a range between 30 and 60° for this angle.
- From the study conducted to verify the range of admissible frequencies, jackets with a high number of braces exhibit greater dispersion in the distribution of the first vibration mode (due to their topological configuration). On the other hand, candidates with fewer braces show less dispersion in the first vibration mode, and these values are close to the 3P limit, indicating the high stiffness of these geometric configurations. It should be noted that jackets with a low number of braces have greater mass, suggesting that stiffness is achieved through an increase in the cross-sectional area or by an increase in the batter angle of the legs. Jacket height remains constant in all cases. Finally, jackets with an intermediate number of braces display higher variability in the fundamental frequency value, confirming that the number of braces is a determining factor in the design.

Among the methodologies and the different strategies proposed in this study for generating initial populations and their subsequent integration into the automatic design and optimization algorithm, developed in Benítez-Suárez et al. (2025), it is confirmed that using ANN optimized pre-computed initial populations enhances both the quantity and quality of the resulting candidates. Among the evaluated approaches, PC-NN-BEST emerges as the most comprehensive, as it yields the high-

est percentage of candidates fulfilling all requirements, has the lowest median computational time, and delivers structurally more efficient solutions in terms of both mass and global compliance factor. The behavior and performance of the proposed methodology have been studied with a focus on specific metocean and soil conditions (described in Table 2) and for the NREL-5 MW OWT (described in Table 1). Future work should address the scalability of the algorithm by analyzing its performance for different metocean and soil conditions, for greater water depths, and for larger turbines.

CRediT authorship contribution statement

Borja Benítez-Suárez: Conceptualization, Formal analysis, Investigation, Methodology, Software, Visualization, Writing – original draft, Writing – review & editing; Román Quevedo-Reina: Conceptualization, Methodology, Software, Writing – review & editing; Guillermo M. Álamo: Conceptualization, Formal analysis, Methodology, Project administration, Supervision, Writing – original draft, Writing – review & editing; Luis A. Padrón: Conceptualization, Formal analysis, Funding acquisition, Methodology, Project administration, Writing – original draft, Writing – review & editing.

Declaration of competing interest

The authors declare that they have no known competing financial interests or personal relationships that could have appeared to influence the work reported in this paper.

Acknowledgements

This research has been funded by Ministerio de Ciencia, Innovación y Universidades and Agencia Estatal de Investigación (MI-CIU/AEI/10.13039/501100011033) of Spain, and ERDF/EU, through research project PID2023-151635OB-I00. In addition, Borja Benítez-Suárez is a recipient of the research fellowship (FPI2024010008) from the program of predoctoral fellowships from the Consejería de Universidades, Ciencia e Innovación y Cultura (Agencia Canaria de la Investigación, Innovación y Sociedad de la Información) of the Gobierno de Canarias and Fondo Social Europeo Plus (FSE+).

References

American Petroleum Institute (API), 2014. API Recommended Practice 2A-WSD: Planning, Designing, and Constructing Fixed Offshore Platforms-Working Stress Design.

Arany, L., Bhattacharya, S., Macdonald, J., Hogan, S.J., 2017. Design of monopiles for offshore wind turbines in 10 steps. Soil Dyn. Earthq. Eng. 92, 126–152.

Arent, D., Sullivan, P., Heimiller, D., Lopez, A., Eurek, K., Badger, J., Jorgensen, H.E., Kelly, M., Clarke, L., Luckow, P., 2012. Improved Offshore Wind Resource Assessment in Global Climate Stabilization Scenarios. Technical Report. National Renewable Energy Lab. (NREL), Golden, CO (United States). https://doi.org/10.2172/1055364

Bahar, H., 2024. Renewables 2023. Analysis and forecast to 2028. Technical Report. International Energy Agency (IEA).

Benítez-Suárez, B., Quevedo-Reina, R., Álamo, G.M., Padrón, L.A., 2025. PSO-based design and optimization of jacket substructures for offshore wind turbines. Mar. Struct. 101, 103759. https://doi.org/10.1016/j.marstruc.2024.103759

Council, G. W.E., 2023. Global Offshore Wind Report 2023. Technical report, GWEC: Brussels, Belgium .

Det Norske Veritas AS, 2019a. DNV-RP-C202: Buckling strength of shells.

Det Norske Veritas AS, 2019b. DNV-RP-C203: Fatigue design of offshore steel structures. Det Norske Veritas AS, 2019c. DNVGL-RP-C205: Environmental Conditions and Environmental Loads.

Det Norske Veritas AS, 2021. DNV-ST-0126: Support structures for wind turbines.

Det Norske Veritas AS, 2024. DNVGL-ST-0437: Loads and site conditions for wind turbines. Det Norske Veritas AS, 2014. DNV-OS-J101 Design of offshore wind turbine structures.

Eberhart, R.C., Shi, Y., 2000. Comparing inertia weights and constriction factors in particle swarm optimization. In: Proceedings of the 2000 Congress on Evolutionary Computation. CEC00 (Cat. No. 00TH8512). Vol. 1. IEEE, pp. 84–88.

Friedman, Z., Kosmatka, J.B., 1993. An improved two-node timoshenko beam finite element. Comput. Struct. 47 (3), 473–481. https://doi.org/10.1016/0045-7949(93) 90243-7

Han, F., Wang, W., Zheng, X.-W., Han, X., Shi, W., Li, X., 2024. Investigation of essential parameters for the design of offshore wind turbine based on structural reliability. Reliab. Eng. Syst. Saf., 110601 https://doi.org/10.1016/j.ress.2024.110601 International Electrotechnical Commission (IEC), 2019. Wind energy generation systems
Part 1: Design requirements.

B. Benítez-Suárez et al.

- Jalbi, S., Bhattacharya, S., 2020. Concept design of jacket foundations for offshore wind turbines in 10 steps. Soil Dyn. Earthq. Eng. 139, 106357. https://doi.org/10.1016/j. soildyn.2020.106357
- Jiang, Z., 2021. Installation of offshore wind turbines: a technical review. Renew. Sustain. Energy Rev. 139, 110576. https://doi.org/10.1016/j.rser.2020.110576
- Johnston, B., Foley, A., Doran, J., Littler, T., 2020. Levelised cost of energy, a challenge for offshore wind. Renew. Energy 160, 876–885. https://doi.org/10.1016/j.renene. 2020.06.030
- Jonkman, J., Butterfield, S., Musial, W., Scott, G., 2009. Definition of a 5-MW Reference Wind Turbine for Offshore System Development. Technical Report. National Renewable Energy Lab. (NREL), Golden, CO (United States).
- Ju, S.-H., Hsieh, C.-H., 2022. Optimal wind turbine jacket structural design under ultimate loads using Powell's method. Ocean Eng. 262, 112271.
- Jung, C., Schindler, D., 2023. The properties of the global offshore wind turbine fleet. Renew. Sustain. Energy Rev. 186, 113667.
- Kennedy, J., Eberhart, R., 1995. Particle swarm optimization. In: Proceedings of ICNN'95-International Conference on Neural Networks. Vol. 4. IEEE, pp. 1942 –1948
- Lu, F., Long, K., Zhang, C., Zhang, J., Tao, T., 2023. A novel design of the offshore wind turbine tripod structure using topology optimization methodology. Ocean Eng. 280, 114607
- Ma, C., Ban, J., Zi, G., 2024. Comparative study on the dynamic responses of monopile and jacket-supported offshore wind turbines considering the pile-soil interaction in transitional waters. Ocean Eng. 292, 116564.
- McCoy, A., Musial, W., Hammond, R., Mulas Hernando, D., Duffy, P., Beiter, P., Perez, P., Baranowski, R., Reber, G., Spitsen, P., 2024. Offshore Wind Market Report: 2024 Edition. Technical Report. National Renewable Energy Laboratory (NREL), Golden, CO (United States). https://www.nrel.gov/docs/fy24osti/90525.pdf.
- Quevedo-Reina, R., 2024. Implementation of ANN-based models to assist in the analysis and design of jacket foundations structures for offshore wind turbines. Ph.D. thesis.

- Quevedo-Reina, R., Álamo, G.M., Aznárez, J.J., 2024a. Estimation of pile stiffness in non-homogeneous soils through artificial neural networks. Eng. Struct. 308, 117999.
- Quevedo-Reina, R., Álamo, G.M., Aznárez, J.J., 2024b. Global sensitivity analysis of the fundamental frequency of jacket-supported offshore wind turbines using artificial neural networks. J. Mar. Sci. Eng. 12 (11), 2011.
- Quevedo-Reina, R., Álamo, G.M., François, S., Lombaert, G., Aznárez, J.J., 2024c. Importance of the soil-structure interaction in the optimisation of the jacket designs of offshore wind turbines. Ocean Eng. 303, 117802.
- Shadlou, M., Bhattacharya, S., 2016. Dynamic stiffness of monopiles supporting offshore wind turbine generators. Soil Dyn. Earthq. Eng. 88, 15–32.
- The MathWorks Inc., 2022. MATLAB version: 9.12.0 (R2022a).
- Tian, X., Liu, G., Deng, W., Xie, Y., Wang, H., 2024. Fatigue constrained topology optimization for the jacket support structure of offshore wind turbine under the dynamic load. Appl. Ocean Res. 142, 103812.
- Vemula, N.K., De Vries, W., Fischer, T., Cordle, A., Schmidt, B., 2010. Design solution for the Upwind reference offshore support structure. Upwind.
- Vorpahl, F., Popko, W., Kaufer, D., 2011. Description of a basic model of the "UpWind reference jacket" for code comparison in the OC4 project under IEA Wind Annex 30.
- Wan, L., Moan, T., Gao, Z., Shi, W., 2024. A review on the technical development of combined wind and wave energy conversion systems. Energy 294, 130885.
- Wang, Z., Mantey, S.K., Zhang, X., 2024. A numerical tool for efficient analysis and optimization of offshore wind turbine jacket substructure considering realistic boundary and loading conditions. Mar. Struct. 95, 103605.
- Zhang, C., Long, K., Zhang, J., Lu, F., Bai, X., Jia, J., 2022. A topology optimization methodology for the offshore wind turbine jacket structure in the concept phase. Ocean Eng. 266, 112974.
- Álamo, G.M., Martínez-Castro, A.E., Padrón, L.A., Aznárez, J.J., Gallego, R., Maeso, O., 2016. Efficient numerical model for the computation of impedance functions of inclined pile groups in layered soils. Eng. Struct. 126, 379–390.